Vermeesch, P., Balco, G., Blard, P.-H., Dunai, T. J., Kober, F., Niedermann, S., Shuster, D. L., Strasky, S., Stuart, F. M., Wieler, R., Zimmermann, L. (2015): Interlaboratory comparison of cosmogenic 21Ne in quartz. - *Quaternary Geochronology*, *26*, p. 20-28.

DOI: http://doi.org/10.1016/j.quageo.2012.11.009

Interlaboratory comparison of cosmogenic ^{21}Ne in quartz

Pieter Vermeesch[a,b], Greg Balco[c], Pierre-Henri Blard[e], Tibor J. Dunai[f], Florian Kober[a], Samuel Niedermann[g], David L. Shuster[d,c], Stefan Strasky[a], Finlay M. Stuart[h], Rainer Wieler[a], Laurent Zimmermann[e]

[a] *Institute of Geochemistry and Petrology, ETH Zurich, Zürich, Switzerland*
[b] *London Geochronology Centre, University College London, London, United Kingdom*
[c] *Berkeley Geochronology Center, Berkeley, United States*
[d] *Department of Earth and Planetary Science, University of California, Berkeley, United States*
[e] *Centre de Recherches Pétrologiques et Géochimiques, Vandoeuvre-lès-Nancy, France*
[f] *University of Cologne, Köln, Germany*
[g] *Deutsches GeoForschungsZentrum GFZ, Potsdam, Germany*
[h] *Scottish Universities Environmental Research Centre, Glasgow, United Kingdom*

Abstract

We performed an interlaboratory comparison study with the aim to determine the accuracy of cosmogenic ^{21}Ne measurements in quartz. CREU-1 is a natural quartz standard prepared from amalgamated vein clasts which were crushed, thoroughly mixed, and sieved into 125-250 μm and 250-500μm size fractions. 50 aliquots of CREU-1 were analyzed by five laboratories employing six different noble gas mass spectrometers. The released gas contained a mixture of 16-30% atmospheric and 70-84% non-atmospheric (predominantly cosmogenic) ^{21}Ne, defining a linear array on the ^{22}Ne/^{20}Ne-^{21}Ne/^{20}Ne three isotope diagram with a slope of 1.108±0.014. The internal reproducibility of the measurements is in good agreement with the formal analytical precision for all participating labs. The external reproducibility of the ^{21}Ne concentrations between labs, however, is significantly overdispersed with respect to the reported analytical precision. We report an average reference concentration for CREU-1 of $348\pm10\times10^6$at[^{21}Ne]/g[SiO_2], and suggest that the 7.1% (2σ) overdispersion of our measurements may be representative of the current accuracy of cosmogenic ^{21}Ne in quartz. CREU-1 was tied to CRONUS-A, which is a second reference material prepared from a sample of Antarctic sandstone. We propose a reference value of $320\pm11\times10^6$at/g for CRONUS-A. The CREU-1 and CRONUS-A intercalibration materials may be used to improve the consistency of cosmogenic ^{21}Ne to the level of the analytical precision.

1. Introduction

Cosmogenic neon is a relatively little used tool for studying Earth surface processes. It is powerful for four reasons. First, it is produced and retained in quartz (Niedermann et al., 1993, 1994; Shuster and Farley, 2005) as well as most other silicates, such as pyroxene (Schäfer et al., 1999), olivine (Poreda and Cerling, 1992), sanidine (Kober et al., 2005), hornblende and biotite (Amidon and Farley, 2012). Therefore, it is applicable to most rock types found on the Earth's surface. Second, cosmogenic ^{21}Ne is a stable nuclide. This gives it an age range limited essentially only by the erosion rate and allows exceptionally old landscapes to be dated (Schäfer et al., 1999; Dunai et al., 2005). Third, neon has three isotopes (^{20}Ne, ^{21}Ne, and ^{22}Ne), each of which have different abundances in the various reservoirs (atmospheric, nucleogenic, or magmatic) that may contribute to the natural ^{21}Ne background (Niedermann, 2002). By simultaneously analyzing all three isotopes and verifying whether they plot on a mixing line between atmospheric and spallogenic components, the cosmogenic neon method provides an internal 'reliability check' which is absent from other commonly used nuclides. Fourth, neon can be measured using a standard sector field noble gas mass spectrometer. Sample requirements are modest (typically 100-200 mg) and sample preparation is relatively straightforward as it does not require extensive chemical purification or chromatography. This greatly increases sample throughput, which in turn opens up exciting opportunities for detrital work (Dunai et al., 2005; Codilean et al., 2008).

Cosmogenic ^{21}Ne is even more useful when combined with one or more cosmogenic radionuclides such as ^{10}Be or ^{26}Al. Such double- or triple-dating may be used for burial dating (Balco and Shuster, 2009a; Vermeesch et al., 2010), for catchment-wide erosion studies with complex exposure histories (Kober et al., 2009), or to measure the exposure age of old and very slowly eroding surfaces (Fujioka et al., 2005). An implicit assumption of many of these studies is that the accuracy of the ^{21}Ne method equals its analytical precision. Violation of this assumption may lead to erroneous results such as samples plotting in the 'forbidden

zone' of the $^{21}Ne/^{10}Be$ two-nuclide diagram (Lal, 1991; Kober et al., 2011). An interlaboratory comparison study was set up in the framework of the CRONUS-EU initiative (Stuart and Dunai, 2009) with the aim to address this issue and provide the noble gas community with a well-characterized reference standard for the analysis of cosmogenic ^{21}Ne in quartz. The CREU-1 standard is a mixture of natural quartz pebbles, rich in cosmogenic ^{21}Ne, which were crushed and thoroughly homogenized to ensure optimal reproducibility (Section 2). Two size-fractions of CREU-1 were analyzed by five prominent cosmogenic noble gas laboratories, each of which used different experimental setups and data reduction protocols (Section 3). In total, 50 aliquots of CREU-1 were analyzed, with reported analytical precisions of 2-6%, but an external reproducibility of 7.1% (Section 4). These analyses were tied to a further 10 measurements of CRONUS-A, which is a second reference material prepared from an Antarctic quartzite analysed by two of the participating labs (Section 5).

2. Standard material

The CREU-1 standard material is pure quartz prepared from exposed vein-quartz clasts of a Miocene erosion surface (19°33'53.4"S, 70°7'1.5"W, 930 m) in the Atacama desert near Pisagua, Chile (between sites B and C of Dunai et al., 2005). The clasts were shed onto the surface from local sources after the main sedimentation episode at ∼12-14 Ma (Dunai et al., 2005). Approximately 400g of material was mixed from five clasts (sample name CH04/5, pebbles 5, 6, 7, 8 and 13, weighing 81g, 104g, 77g, 109g and 55g respectively) that had ^{21}Ne excess concentrations within 5% of their mean value. After crushing in a W-carbide disk mill, five size fractions were prepared using stainless steel sieves:

- 40-62μm: 10.45g, wet sieved and dried overnight at 50°C
- 63-125μm: 40.62g, wet sieved and dried overnight at 50°C
- 125-250μm: 74.4g, dry sieved
- 250-500μm: 188g, dry sieved

- >500μm: 15.8g, dry sieved

Of these five fractions, the 125-250μm and 250-500μm fractions were taken to produce the standard material, while the remaining fractions were preserved, but not processed any further. The 125-250μm and 250-500μm fractions were soaked in concentrated sulfuric acid at 120°C overnight, to remove all iron coatings and accessory minerals such as rutile, sphene and fluorite. After the acid treatment, the material was rinsed ten times in cold de-ionized water, followed by five times one hour ultrasonic rinsing in de-ionized water at 80°C. Next, the quartz was dried overnight at 110°C. Although the preparation steps outlined above probably already ensured a thoroughly mixed quartz sand, a FRITSCH® rotary cone sample divider laborette 27 was used to split the material into 16 equal fractions. Different aliquots of CREU-1 have been analyzed by five noble gas laboratories, at BGC (Berkeley), CRPG (Nancy), ETH (Zürich), GFZ (Potsdam) and SUERC (Glasgow).

3. Analytical methods

The five participating laboratories employed a variety of noble gas mass spectrometers and analytical procedures for cosmogenic ^{21}Ne analysis. Rather than forcing all the participants to use the same heating schedules, gettering times and so forth, they were allowed to use their own measurement routines, so that the calibration exercise fully captured the diversity of approaches used for ^{21}Ne analysis. The temperature steps and amount of material used are reported in Tables 1-3.

3.1. BGC

Neon extraction from quartz at BGC employed a 14-sample vacuum chamber with a 3 inch diameter sapphire viewport. Samples of up to 150 mg quartz were encapsulated in a Ta packet and heated through the viewport by a 150 W diode laser (λ = 810 nm) using a feedback control system in which the temperature of the packet was continuously monitored by an optical pyrometer coaxial with the laser delivery optic. Calibration of the pyrometer for the emissivity of the Ta packets was accomplished by placing a thermocouple in the

same apparatus. Collateral heating of adjacent samples was prevented by completing one heating step for all samples before beginning the next heating step. This procedure was tested by interspersing blanks consisting of an empty Ta packet. After heating, sample gas was reacted with a SAES® getter and adsorbed to a cryogenic trap at 20 K. Neon was then released into the mass spectrometer at 70 K. All sample heating, gas processing, and measurement operations were automatically controlled. Analyses were done with a MAP-215 mass spectrometer updated with modern ion-counting electronics. Under normal operating conditions, this machine had a relatively low Ar^+/Ar^{++} ratio (2.5-5, depending on source tuning) and inadequate mass resolution to fully resolve $^{20}Ne^+$ from $^{40}Ar^{++}$, so a correction for background $^{40}Ar^{++}$ was required. As described in Balco and Shuster (2009b), this was accomplished by introducing a ^{39}Ar spike and monitoring the Ar charge ratio as well as the $^{40}Ar^+$ signal throughout each analysis. The resulting correction on mass 20 varied between analyses, but was typically equivalent to $5.00 \pm 0.02 \times 10^8$ atoms ^{20}Ne. Similarly, a correction for $^{12}C^{16}O_2^{++}$ on mass 22 was made by establishing a relationship between the Ar and CO_2 charge ratios. Absolute calibration of Ne abundance was made by peak height comparison against an air standard processed in the same way as the samples and analyzed several times daily. Linearity of machine response was verified by varying the volume of the air standard. The pressure of the air standard reservoir was measured during loading with an MKS Baratron manometer, and corrected for atmospheric water vapor using three separate hygrometers at the time of air sample collection. Absolute volumes of the reservoir and pipette were determined by differential pressure measurements, again using the Baratron, against two separate reference glass ampules whose volumes were independently measured by Hg weighing. The amount of cosmogenic ^{21}Ne was calculated by assuming two-component mixing of atmospheric and cosmogenic neon. Reported uncertainties include i) counting uncertainties on all masses, including those used to generate corrections for $^{40}Ar^{++}$ and CO_2^{++}; ii) uncertainty in blank subtraction (the ^{21}Ne process blank was $\sim$ 0.5 Hz or $\sim$ 90,000 atoms, which was $< 1\%$ of typical signals on mass 21 for these measurements); and iii) the reproducibility of the air standards ($\sim$1% for ^{20}Ne, $\sim$3% for ^{21}Ne).

3.2. CRPG

After 10 minutes cleaning in an acetone ultrasonic bath, quartz aliquots were wrapped in copper foils (Alfa Aesar®, 0.025 mm thick, 99.8%). Samples were then loaded under high vacuum in a stainless steel carousel that had been baked during 10 h at 80°C. Gas extraction from the quartz was realized by 25 minutes heating in a home-designed single vacuum resistance furnace with a boron nitride crucible (Zimmermann et al., in press). Sequential purification with charcoals in liquid nitrogen, titanium sponges (JohnsonMatthey®, mesh m3N8 t2N8) and SAES® getters (ST172/HI/20-10/650C) permitted gas cleaning by removal of H_2O, Ar, Kr, Xe and hydrocarbons. Ne was not separated from He. The purified gas was finally analyzed using a VG5400 mass spectrometer. Corrections for isobaric interferences of $^{40}Ar^{++}$ at m/e = 20 and $^{12}C^{16}O_2^{++}$ at m/e = 22 were negligible compared to the amount of analyzed neon. The mass spectrometer sensitivity was determined by peak height comparison against a 0.2 cm^3 ($\sim 1.6\times10^{10}$ atoms of ^{20}Ne) pipette of a gas standard having an atmospheric composition. Typical furnace blanks at 1000-1300°C (25 min) were $1.0\pm0.2\times10^8$, $3\pm1\times10^5$ and $1.63\pm0.06\times10^7$ atoms of ^{20}Ne, ^{21}Ne and ^{22}Ne, respectively. Excess ^{21}Ne ($^{21}Ne^*$) concentrations were calculated following:

$$^{21}Ne^* = R_c \times^{20} Ne_m \times (R_m - R_a)/(R_c - R_a) \quad (1)$$

where $^{20}Ne_m$ is the measured ^{20}Ne, R_c is the cosmogenic $^{21}Ne/^{20}Ne$-ratio ($R_c = 0.8$; Niedermann, 2002), R_m is the measured $^{21}Ne/^{20}Ne$-ratio, and R_a is the atmospheric $^{21}Ne/^{20}Ne$-ratio ($R_a = 0.00296$).

3.3. ETH

Noble gases were extracted by heating in a molybdenum crucible. Released gases were cleaned in a stainless steel extraction line equipped with Al/Zr-getters (SAES®) and activated charcoal held at the temperature of liquid nitrogen before He and Ne were expanded to a cryogenic pump. Helium and neon were separated by adsorbing neon at 14 K on stainless steel frits and analyzing helium first. After pumping away the helium, neon was released

from the cryotrap at 50 K. Noble gas analyses were performed in a custom-made, all-metal magnetic sector mass-spectrometer (90°, 210 mm radius) equipped with a modified Baur-Signer ion source with essentially constant sensitivity over the pressure range relevant for this work (Baur, 1980). The ion source was equipped with a compressor device increasing the sensitivity by factors of 120 and 200 for ^{3}He and ^{21}Ne, respectively (Baur, 1999) compared to the sensitivities of the same spectrometer with the compressor turned off. The absolute sensitivity and mass discrimination of the mass spectrometer were determined by analysing known amounts of standard noble gas mixtures prepared from commercially available pure gases. The Ne isotopic composition of the standard gas was cross calibrated against two air standards (Heber et al., 2009). Similarly, the Ne amounts delivered by the standard pipette were cross calibrated with air standards as well as with other independently filled standard gas bottles. The uncertainty of the Ne standard gas amounts is estimated to be 2% (Heber et al., 2009). Full procedural blanks (45' at 600^{o}C + 20' at 800° + 15' at 1750°C) were $1.211\pm0.006\times10^{8}$, $3.5\pm0.2\times10^{5}$, and $1.17\pm0.01\times10^{7}$ atoms of ^{20}Ne, ^{21}Ne and ^{22}Ne, respectively. Corrections for isobaric interferences on mass 20 have been applied for $^{40}Ar^{++}$ and $H_2^{18}O^{+}$ but were always less than 2%. No correction for CO_2^{++} on ^{22}Ne was necessary. The low correction factors for doubly charged species were the results of a low electron acceleration voltage of 45V in the ion source. Excess ^{21}Ne (^{21}Ne*) concentrations were calculated with Equation 1.

3.4. GFZ

CREU-1 quartz samples were wrapped in aluminium foil and loaded in a sample carousel without further treatment, except for two aliquots of the 250-500μm fraction (GFZ-6-7) which were crushed to $\sim$50μm grain size in an agate mortar before loading. Noble gases were extracted in a resistance-heated furnace equipped with a tantalum crucible and molybdenum liner and analyzed in either of two VG5400 noble gas mass spectrometers, with measurements GFZ1-7 being measured on one machine, and GFZ8-11 on the other (Tables 1 and 2). GFZ-8 was not heated, but instead crushed in vacuo between two hard metal jaws in order to test whether Ne trapped in fluid inclusions of CREU-1 has an atmospheric isotopic composition.

Gas purification involved a dry ice trap, two titanium sponge and foil getters, and two SAES® (Zr-Al) getters. The noble gases were trapped on stainless steel frits and/or activated charcoal in cryogenic adsorbers and sequentially released for He, Ne, and Ar-Kr-Xe analysis. Isobaric interferences of $^{40}Ar^{++}$ at m/e=20 (up to 20% at 400°C) and $^{12}C^{16}O_2^{++}$ at m/e=22 (up to 10% at 400°C) were corrected according to the method described by Niedermann et al. (1993, 1997). A correction for $H_2^{18}O^+$ at m/e=20 was not necessary due to the mass resolution of ≥600. Blanks had an atmospheric composition and contained 1-3×10^7 atoms of ^{20}Ne, depending on temperature. Excess ^{21}Ne was calculated without applying a blank correction, assuming an atmospheric origin of all the measured ^{20}Ne:

$$^{21}Ne^* = ^{21}Ne_m \times (R_m - R_a)/R_m \quad (2)$$

with all abbreviations as in Equation 1. In some cases a high atmospheric Ne memory (i.e., rapid decay of non-atmospheric Ne isotope ratios) required the application of a special procedure to derive the Ne concentration and isotopic composition at the time of gas admission to the mass spectrometer (see Goethals et al., 2009). Absolute noble gas concentrations were obtained by peak height comparison against a 0.1 cm^3 pipette of calibration gas (an artificial mixture of the five noble gases in nitrogen provided by Linde company; Niedermann et al., 1997), which was cross-calibrated in the 1990s against glass ampoule noble gas standards made available by O. Eugster (University of Bern) and whose noble gas concentrations are judged accurate to ∼3% at 95% confidence level, and have been propagated into the overall uncertainty.

3.5. SUERC

The clean quartz was thoroughly rinsed in ultra-pure acetone and packed into aluminium foil cylinders. Cosmogenic Ne was extracted by heating each sample packet for 20 minutes. The active gases were removed by exposure to two hot SAES® (Zr-Al) getters during heating, and for a further 20 minutes as the furnace cooled. The heavy noble gases and residual active gases were subsequently adsorbed on liquid nitrogen cooled activated charcoal for 10 minutes and exposed to a getter at room temperature to adsorb hydrogen. Neon was then

adsorbed on activated charcoal in a cryostatic cold head at 30K. The helium was pumped for 1 minute, then the Ne was desorbed from the charcoal trap at 100K. Neon isotopes were analyzed statically in a MAP-215 magnetic sector mass spectrometer equipped with a modified Nier-type ion source, an axial electron multiplier (Burle Channeltron) operated in pulse-counting mode and a Faraday detector. A room temperature SAES® G50 getter and a liquid nitrogen-cooled activated charcoal trap were used to minimize the contribution of interfering species during analysis. The data presented here were taken over a period of two years. Consequently source conditions changed to a small degree. Typically the source was tuned for Ne sensitivity prior to analytical periods; electron voltage of 88 V, trap current of 500 μA and an acceleration voltage of 3 kV. A slit in front of the electron multiplier was used to achieve a resolving power (m/Δm) of approximately 400. For all samples and calibrations the abundances of masses 18, 19, 20, 21, 22, 40 and 44 were determined by integrating counts recorded in 40-100 blocks of 5 seconds each. Peak heights of masses 2 and 16 were measured on the Faraday detector. Instrumental sensitivity was calculated from repeated analysis of aliquots of 2.2×10^{10} atoms ^{20}Ne in air sampled from a 5 liter reservoir. Isotopic mass discrimination was approximately 0.50 $\pm$ 0.03 %/amu. The average high temperature ^{20}Ne blank was 1×10^{8} atoms. There was no observed increase when empty Al foil was heated. The Ne isotopic composition of blank measurements after correction for interfering species (see below) was indistinguishable from air ratios. Since it is likely that a significant amount of air-derived Ne is released from the quartz during heating, no blank correction has been made to the data. Excess ^{21}Ne concentrations were calculated assuming an atmospheric origin of all the measured ^{20}Ne according to Equation 2. Interference at m/e = 20 from $H_2^{18}O^+$ was calculated from measurement of $H_2^{16}O^+$ at mass 18. The contribution never exceeded 0.03%. No $H^{19}F^+$ signal was observed in blanks and mass spectrometer backgrounds. The dominant interference at m/e = 20 came from $^{40}Ar^{++}$. The charge state ratio $^{40}Ar^+/^{40}Ar^{++}$ is governed by the partial pressure of H in the mass spectrometer ionization region. A first-order relationship between $^{40}Ar^+/^{40}Ar^{++}$ and H^+ beam size was recorded. The partial pressure of H remained constant resulting in $^{40}Ar^+/^{40}Ar^{++}$ = 2.30-2.32. The contribution

of $^{40}Ar^{++}$ to the measured ^{20}Ne signal in CREU quartz samples was <1%. Correction for $^{12}C^{16}O_2^{++}$ at m/e = 22 was calculated from measured mass 44 ($^{12}C^{16}O_2^{+}$) using a CO_2^+/CO_2^{++} = 50 to 58 (determined by repeated measurements interspersed with sample measurements). No pressure dependence on the CO_2^+/CO_2^{++} ratio was recorded for a 50-fold variation in the partial pressure of H and CO_2. Correction for interfering $^{12}C^{16}O_2^{++}$ never exceeded 1%.

4. Results

All five labs reported data for the coarse fraction, while three labs measured the fine fraction as well. The results for both sets of analyses are reported in Tables 1 and 2. The $^{21}Ne/^{20}Ne$ and $^{22}Ne/^{20}Ne$ compositions of the individual heating steps and their sums are consistent with a predominantly spallogenic origin of the released ^{21}Ne (Figure 1). The pooled analyses comprise 16-30% atmospheric and 70-84% excess ^{21}Ne, with individual heating steps containing up to 98% excess ^{21}Ne. Linear regression of the spallation line yields a slope of 1.108 ± 0.014 (2σ), which is in statistical agreement with previously published values (Table 8 of Niedermann, 2002).

The total excess ^{21}Ne contents of all the aliquots are shown in Figure 2. The reported 2σ analytical uncertainties are between 2 and 6%. The MSWD (Mean Square of the Weighted Deviates, a.k.a. 'reduced Chi-square', McIntyre et al., 1966) is reasonably close to unity for ETH, GFZ and BGC, indicating good agreement of the observed scatter with the measurement errors. The extremely low MSWD of 0.005 for CRPG may indicate overestimated analytical uncertainties, but could also be due to chance, as only two aliquots were analyzed. Finally, the coarse fraction of SUERC is characterized by an MSWD of 4.1, which may indicate underestimated analytical uncertainties. However, measurements of the fine fraction by the same lab have an MSWD of 1.3. There is no systematic difference between the fine and the coarse grain size fractions of ETH, SUERC and GFZ. Measurements GFZ-6-7 were performed on material from the coarse fraction that was crushed for 5 minutes in air with an agate mortar to ∼50μm, resulting in some loss of excess ^{21}Ne. GFZ-8 was crushed in vacuo,

and the data shown are for that crushing extraction. The ^{21}Ne excess of GFZ-8 is considerably less than the ^{21}Ne deficit in GFZ-6-7, probably because the in-vacuo crusher was much less efficient than the mortar. Measurements GFZ-6-8 were not included in subsequent calculations and figures. Total ^{3}He concentrations measured at GFZ were $204\pm10\times10^{6}$at/g for the coarse fraction (seven measurements) and $109\pm7\times10^{6}$at/g (a single analysis) for the fine fraction. The resulting $^{21}Ne/^{3}He$-ratios are significantly greater than the production-rate ratio. This is likely caused by a combination of helium loss due to hot acid etching during sample preparation, and the fact that helium is not quantitatively retained in quartz at surface temperatures (Shuster and Farley, 2005).

BGC analyzed material from two different vials of CREU-1, thus presenting an opportunity to verify the homogeneity of the standard. Measurements BGC-1-4 were performed on material from the same vial as ETH, whereas measurements BGC-5-8 were done on the same vial as CRPG. The observed difference between the two vials analyzed by BGC falls within the analytical uncertainty. The difference between the results of BGC and ETH/CRPG, however, falls well outside the statistically acceptable range. The error-weighted means of all the labs do not agree with each other within the analytical uncertainties, defined as the standard errors of those means. Therefore, in order to calculate a global average of all the data (using both the fine and the coarse grain fractions), we used a random effects model with two sources of uncertainty. We assume that the intra-laboratory averages x_i (where i is an identifier for each participating lab) come from a normal distribution of the form:

$$x_i \sim N(\mu, \sigma_i^2 + \zeta^2) \tag{3}$$

where μ is the global mean, σ_i^2 the analytical uncertainty (variance) of the ith lab, and ζ^2 is the amount of *overdispersion*, i.e. the excess scatter (variance) that cannot be explained by the analytical uncertainty alone. To understand this formula, consider the following two special cases. If $\sigma_i = 0$ (perfect reproducibility within each lab) then μ is the arithmetic mean of the laboratory averages. And if $\zeta = 0$ (perfect reproducibility between all labs) then

μ is the error-weighted mean of those same laboratory averages. In order to simultaneously take into account the finite analytical precision of each lab and the variance between the labs, Equation 3 was iteratively solved for both μ and ζ, yielding an average ^{21}Ne concentration of 348±10×10^{6}at/g and an overdispersion (defined as $2\zeta/\mu$) of 7.1%.

5. Comparison with CRONUS-A

In addition to CREU-1, two of the participating labs also analyzed CRONUS-A as a second reference material. CRONUS-A was collected in Antarctica's Arena Valley (77° 52' 58.9"S, 160° 56' 35.1"E, 1666m elevation), from a large (40kg) yet thin (∼2cm) slab of Beacon sandstone. Quartz was purified at the University of Vermont by crushing, sieving and repeated etching in dilute HF, using procedures designed for cosmogenic ^{10}Be-^{26}Al analysis. CRPG reported one and BGC a further nine analyses of CRONUS-A, using the same protocols that were used for the CREU-1 measurements (Table 3). The average cosmogenic ^{21}Ne content of the nine CRONUS-A samples measured by BGC was 338.9±3.8×10^{6}at/g, i.e. 7.6±3.7% lower than that of CREU-1. The single CRONUS-A analysis of CRPG is lower than its CREU-1 measurements by a similar amount (4±17%), although the reported analytical precision of the latter estimate is much poorer. Additionally, published CRONUS-A values have been reported by two laboratories which did not participate in the interlaboratory comparison, at Harvard University (330±3×10^{6}at/g, Middleton et al., 2012) and the California Institute of Technology (338±10×10^{6}at/g, Amidon and Farley, 2012). Normalizing the average CRONUS-A value reported by BGC to the CREU-1 reference value results in a ^{21}Ne concentration of 320±11×10^{6}at/g. We propose that when this value is used as a reference, CRONUS-A can serve as an alternative to CREU-1.

6. Discussion

It is interesting to note that significant amounts of excess ^{21}Ne remained trapped in the quartz after the second highest heating step, at temperatures of up to 820°C. Total degassing was not achieved until the final temperature step at 1140°C and more. This is significantly

higher than the 800°C release temperature for cosmogenic neon reported by Niedermann (2002). Nevertheless, for all samples of all labs, the data points of the higher temperature steps plot on the mixing line between atmospheric and cosmogenic neon (Figure 1), which strongly suggests that the non-atmospheric neon in all samples is essentially purely cosmogenic, although quartz occasionally also contains a nucleogenic neon component released at high temperature with a $^{21}Ne/^{22}Ne$ ratio of approximately unity (Ne_{HT}, Niedermann et al., 1994; Niedermann, 2002). However, in view of the position of all data points in Figure 1 it seems very improbable that a sizeable fraction of the non-atmospheric ^{21}Ne in our samples could be nucleogenic Ne_{HT}. Even in this unlikely case this would be largely irrelevant for the purpose of interlaboratory comparison, because for all samples we sum the non-atmospheric ^{21}Ne from all temperature steps.

Despite the fact that CREU-1 is pure and highly enriched in spallogenic neon, the ^{21}Ne concentrations reported by the participating labs are significantly overdispersed with respect to the formal analytical uncertainty. In theory, this overdispersion could be due to inhomogeneity of the standard material itself, as different labs analyzed aliquots from different vials of CREU-1. However, the analysis of two of these vials by BGC, and comparison with measurements of those same vials by ETH and CRPG, shows that this is not the case. Therefore, CREU-1 is homogenous. If the overdispersion cannot be attributed to the standard material itself, then it must be due to biases introduced by the different standard calibration bottles used (Heber et al., 2009), or to differences in the neon sensitivity between samples and standards introduced by sample processing or tuning conditions.

7. Conclusion

Our calibration experiment has shown that, although the reported analytical precision of cosmogenic noble gas measurements may be as low as 2%, the accuracy is not quite as good. We suggest that the 7.1% dispersion observed in our study be used as a more realistic estimate of the accuracy of the ^{21}Ne method at the present time. It should be borne in mind that this may even be an optimistic value, for a highly enriched and well behaved standard

material. Using realistic and conservative analytical uncertainties is especially important for studies combining ^{21}Ne with other (radio)nuclides, and to assess the resolving power of such studies. For single nuclide studies, CREU-1 or CRONUS-A measurements can be used to normalize ^{21}Ne to the reference values reported in this paper, so that measurements from different labs can be compared on an equal footing and relative differences in ^{21}Ne can be compared on the level of the analytical precision (Dunai and Stuart, 2009). Those interested in obtaining aliquots of these standards may contact T. Dunai (`tdunai@uni-koeln.de`) for CREU-1 or T. Jull (`jull@email.arizona.edu`) for CRONUS-A.

Acknowledgments

This research was funded by CRONUS-EU (Marie Curie RTN project 511927). We would like to thank Mark Kurz and an anonymous reviewer for positive and constructive feedback on the submitted manuscript.

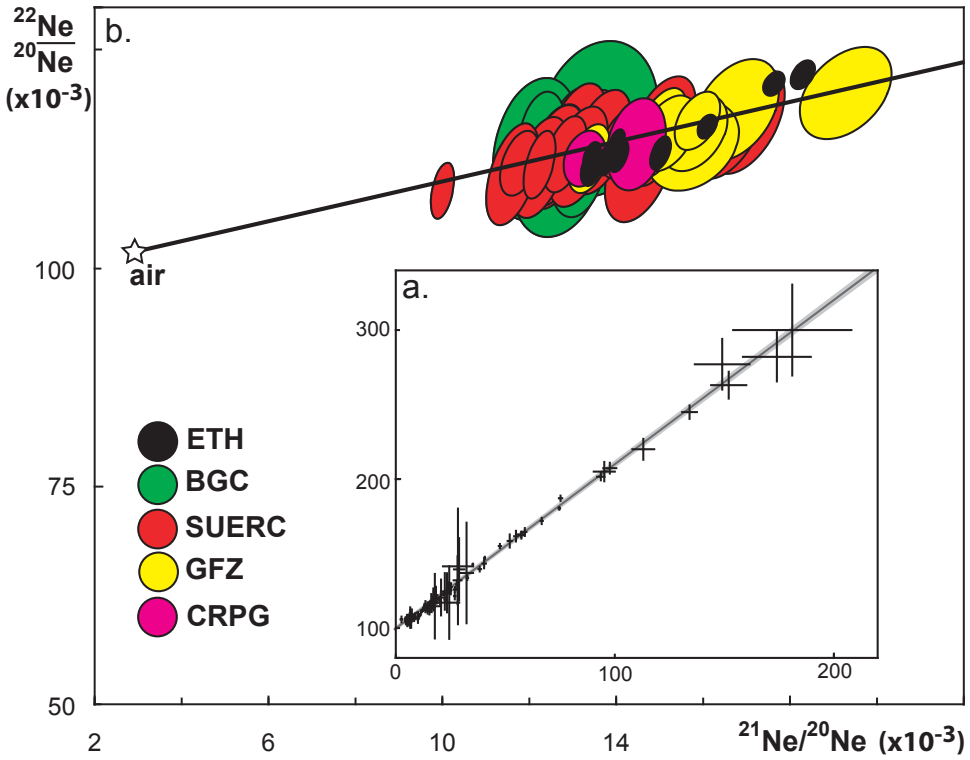

Figure 1: Neon three-isotope plots of (a) all the individual heating steps and (b) the total released gas for each analyzed CREU-1 aliquot. The data fit a spallation line with a slope of 1.108 ± 0.014 (2σ, MSWD = 3.4). Error symbols are 1σ.

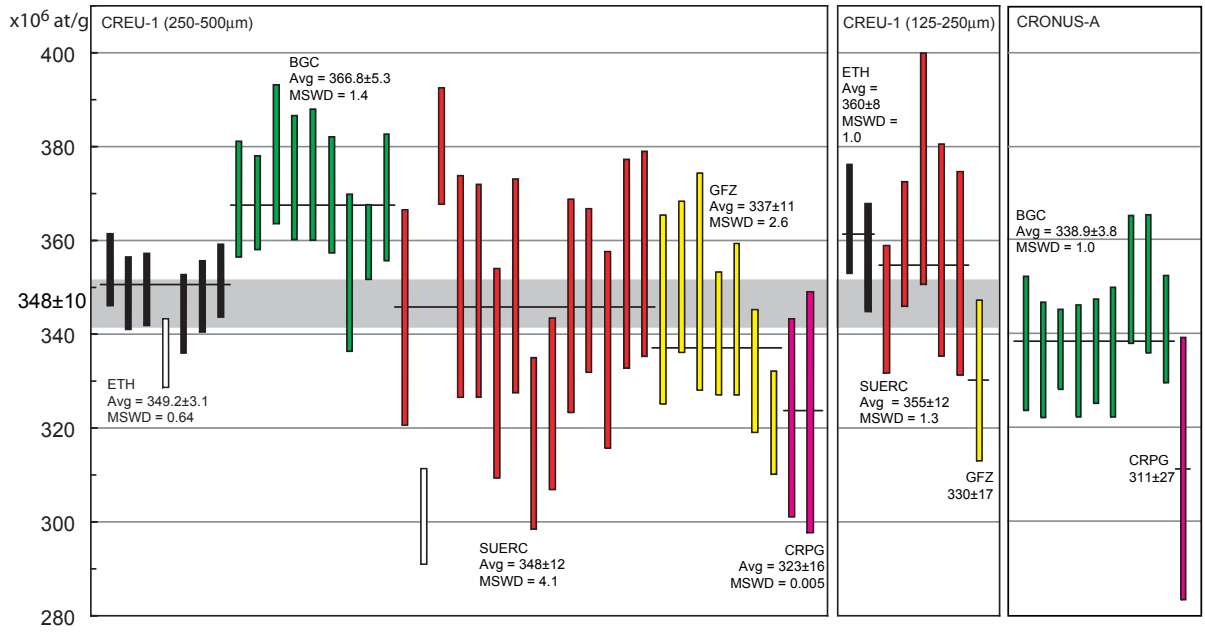

Figure 2: Overview of all the reported ^{21}Ne concentrations and 2σ uncertainties, with indication of the error-weighted means for each participating laboratory. White bars are considered outliers and were not used to calculate the averages. Left and middle panels: coarse and fine fractions of CREU-1; right panel: CRONUS-A. Gray band marks the average and 2σ uncertainty of CREU-1.

Table 1: Summary table of the coarse fraction of CREU-1. '21/20' and '22/20' are the $^{21}Ne/^{20}Ne$ and $^{22}Ne/^{20}Ne$ ratios, ^{21}Ne* is excess ^{21}Ne. Temperatures of ETH-4-7 (marked by an asterisk) and SUERC-8-9 (omitted) were set when the crucible was really full causing samples to be degassed at positions where the temperature was lower than the nominal crucible temperature. GFZ-6-7 were crushed to small grain size ($\sim$50μm) before loading, while GFZ-8 was degassed by in vacuo crushing instead of heating. These samples were not included in Figures 1 and 2.

	mass	T	^{20}Ne	2σ	21/20	2σ	22/20	2σ	^{21}Ne*	2σ	sum	2σ
	[mg]	[°C]	[$\times 10^9$at/g]		[$\times 10^{-3}$]		[$\times 10^{-3}$]		[$\times 10^6$at/g]		[$\times 10^6$at/g]	
ETH-1	66.37	600	13.37	0.27	24.23	0.15	126.61	0.83	285.5	6.1		
		800	9.85	0.20	6.96	0.11	105.59	0.67	39.6	1.0		
		1750	8.70	0.19	6.22	0.10	106.57	1.00	28.4	0.8	353.5	7.6
ETH-2	66	600	11.45	0.24	27.78	0.26	129.17	0.74	285.1	6.5		
		800	8.42	0.17	7.52	0.13	106.92	1.30	38.6	1.0		
		1750	6.62	0.18	6.70	0.14	105.90	0.98	24.9	0.8	348.5	7.7
ETH-3	49.23	800	22.13	0.45	17.15	0.13	117.11	0.29	315.3	6.9		
		1750	11.16	0.22	5.99	0.12	104.81	1.15	34.0	0.9	349.2	7.6
ETH-4	82.13	600*	1.34	0.03	74.66	0.76	180.3	1.9	96.3	2.4		
		800*	1.39	0.15	26.91	0.56	125.9	3.1	33.4	3.6		
		1750*	25.18	0.50	11.16	0.11	109.0	1.2	207.3	4.7	335.8	7.3
ETH-5	48.56	600*	1.89	0.04	47.5	1.0	155.0	2.7	84.7	2.6		
		800*	1.58	0.28	22.44	0.42	119.2	2.3	30.9	5.5		
		1750*	29.42	0.59	10.74	0.17	108.4	1.8	229.8	5.8	344.2	8.3
ETH-6	48.73	600*	1.43	0.03	66.6	1.0	171.9	4.2	91.5	2.6		

Continued on next page

Table 1 – continued from previous page

	mass	T	^{20}Ne	2σ	21/20	2σ	22/20	2σ	^{21}Ne*	2σ	sum	2σ
		800*	2.21	0.15	24.18	0.55	124.2	1.7	47.1	3.3		
		1750*	28.54	0.57	10.31	0.10	108.6	1.0	210.5	4.7	347.8	7.6
ETH-7	81.3	600*	1.39	0.03	75.2	1.5	187.1	3.5	100.8	3.0		
		800*	1.75	0.13	27.37	0.42	126.4	2.1	42.8	3.3		
		1750*	28.56	0.57	10.24	0.09	108.5	0.7	208.8	4.5	351.2	7.7
BGC-1	109.9	370	4.1	1.5	24.4	9.1	117	49	86.9	6.0		
		740	14.0	0.9	17.3	1.2	119	11	200.0	7.7		
		1140	20.3	1.3	7.0	0.5	105	8	81.5	7.4	368	12
BGC-2	129.4	370	5.3	0.8	22.4	3.6	125	25	101.6	5.2		
		740	15.0	0.5	15.9	0.6	114	7	194.9	7.4		
		1140	19.0	0.6	6.8	0.3	105	5	71.1	4.2	368	10
BGC-3	115.7	390	4.7	0.6	28.2	3.6	132	32	121.3	6.9		
		780	19.8	1.6	13.5	0.7	114	7	210	12		
		1140	12.7	0.5	6.7	0.4	109	6	46.5	4.1	378	15
BGC-4	104.8	390	5.8	0.7	23.4	3.0	124	26	119.6	8.1		
		780	16.5	0.9	15.4	0.9	113	8	203.4	8.6		
		1140	14.9	1.0	6.6	0.5	105	10	50.1	5.7	373	13
BGC-5	103.5	370	3.1	0.6	32.3	6.0	137	67	90.7	6.9		
		740	14.2	0.7	17.1	0.8	121	12	203.4	9.6		
		1140	22.7	1.2	6.5	0.3	108	5	79.6	7.5	374	14
BGC-6	83.2	370	3.5	1.7	28	14	141	78	87.2	6.9		
		740	12.9	0.8	18.3	1.2	122	11	201.9	7.8		
		1140	18.2	1.0	7.3	0.5	109	7	80.3	6.5	369	12
BGC-7	75	390	6.3	2.0	17.8	5.7	115	43	92.4	8.6		

353 Continued on next page

Table 1 – continued from previous page

	mass	T	^{20}Ne	2σ	21/20	2σ	22/20	2σ	^{21}Ne*	2σ	sum	2σ
		780	15.3	1.0	16.2	1.1	118	10	199	13		
		1140	17.6	0.9	6.6	0.4	110	8	61.8	6.1	353	17
BGC-8	144.4	390	5.9	1.0	20.7	3.3	121	24	103.4	5.6		
		780	15.3	0.5	16.0	0.6	115	5	196.3	4.4		
		1140	17.2	0.6	6.5	0.2	106	4	59.7	3.5	359	8
BGC-9	110.2	370	3.9	0.6	28.9	4.8	139	42	101.7	5.8		
		740	14.0	0.8	17.2	1.0	117	10	202	11		
		1140	18.9	0.6	6.6	0.3	108	5	65.5	5.3	369	13
SUERC-1	165.1	1350	30.2	1.8	14.50	0.38	111.5	3.5	343	23	343	23
SUERC-2	239.6	480	1.82	0.11	24.12	0.80	127.8	5.8	37.9	2.7		
		550	1.02	0.06	40.3	1.6	143.3	6.4	37.8	3.0		
		650	3.67	0.22	20.21	0.61	118.2	5.2	62.4	4.4		
		800	8.55	0.51	15.88	0.45	116.0	4.8	108.9	7.4		
		1400	18.0	1.1	6.02	0.14	105.2	3.9	54.2	3.5	301	10
SUERC-3	258.4	480	4.91	0.29	25.10	0.67	125.4	5.5	107.3	7.2		
		550	5.31	0.32	25.20	0.71	127.6	5.1	116.5	7.9		
		650	2.79	0.17	16.40	0.63	113.5	5.4	37.0	2.9		
		800	11.33	0.68	8.34	0.27	106.9	4.4	60.1	4.3		
		1200	14.73	0.88	6.20	0.17	104.7	4.4	47.0	3.2		
		1350	5.24	0.31	5.24	0.19	103.7	4.8	11.8	0.9	380	12
SUERC-4	203	1350	36.5	2.2	12.57	0.32	112.8	2.3	350	23	350	23
SUERC-5	204.6	1350	33.8	2.0	13.32	0.30	114.4	2.3	349	23	349	23
SUERC-6	261.3	1350	32.9	2.0	13.06	0.33	115.1	2.3	332	22	332	22
SUERC-7	160.2	1350	40.6	2.4	11.59	0.23	110.8	1.6	350	23	350	23

Continued on next page

Table 1 – continued from previous page

	mass	T	^{20}Ne	2σ	21/20	2σ	22/20	2σ	^{21}Ne*	2σ	sum	2σ
SUERC-8	237.3	-	17.7	1.1	19.33	0.33	119.5	1.5	289	18		
		-	4.95	0.30	6.27	0.26	106.3	3.8	16.3	1.2		
		-	3.17	0.19	5.12	0.16	104.1	1.3	6.8	0.5		
		-	2.53	0.15	4.86	0.17	106.6	1.8	4.8	0.4	317	18
SUERC-9	196.1	-	21.1	1.3	16.72	0.28	117.2	0.9	289	18		
		-	6.53	0.39	5.75	0.10	105.0	0.8	18.1	1.1		
		-	6.16	0.37	5.14	0.14	105.4	1.3	13.4	0.9		
		-	3.45	0.21	4.40	0.20	105.8	1.5	4.9	0.4	325	18
SUERC-10	175.4	1350	35.4	2.1	12.79	0.27	113.1	0.9	346	23		
		1350	0.81	0.05	2.60	0.85	105.8	3.8	-	-	346	23
SUERC-11	209.2	1350	11.88	0.71	25.00	0.44	126.3	1.1	260	16		
		1350	23.8	1.4	6.70	0.13	106.5	0.8	88.7	5.7	349	17
SUERC-12	187.8	1350	32.5	1.9	13.33	0.21	113.0	0.8	335	21		
		1350	0.88	0.05	4.45	0.43	105.5	3.4	1.3	0.2	336	21
SUERC-13	202.3	1350	33.5	2.0	13.59	0.22	114.5	0.8	355	22	355	22
SUERC-14	92.8	1350	39.7	2.4	12.22	0.12	111.5	0.5	357	22	357	22
GFZ-1	50.56	400	0.7	0.13	149	25	277	34	99.4	9.5		
		800	18.6	1.3	15.04	0.47	115.6	2.1	224	17		
		1200	5.7	0.47	6.70	0.41	107.4	4.5	21.2	2.6	345	20
GFZ-2	102.5	400	1.1	0.14	95.2	9.6	205	13	105.1	8.3		
		800	16.2	1.0	15.88	0.34	115.8	1.2	209	13		
		1200	11.3	0.73	6.32	0.12	105.9	1.4	38.1	2.6	352	16
GFZ-3	99.58	400	0.4	0.14	181	54	300	61	72.8	6.7		
		800	15.2	1.1	18.72	0.95	117.1	1.2	239	22		

Continued on next page

Table 1 – continued from previous page

	mass	T	^{20}Ne	2σ	21/20	2σ	22/20	2σ	^{21}Ne*	2σ	sum	2σ
		1200	11.8	0.84	6.33	0.19	103.4	1.2	39.6	3.5	351	23
GFZ-4	100.4	400	0.7	0.08	113	10	220	14	76.2	4.9		
		800	21.1	1.1	13.82	0.14	113.1	3.3	229	12		
		1200	10.8	0.58	6.22	0.20	104.5	0.8	35.2	2.9	340	13
GFZ-5	104.52	400	0.5	0.09	174	31	282	33	79.8	7.2		
		800	16.7	1.0	16.77	0.30	115.3	0.8	231	14		
		1200	9.4	0.56	6.42	0.18	107.5	1.3	32.5	2.5	343	16
GFZ-6	101.26	400	1.1	0.10	216	14	335	13	239	19		
		800	2.6	0.20	25.21	0.93	126.2	4.8	57.0	4.0		
		1200	0.1	0.06	4.20	4.40	90	35	0.1	0.2	296	19
GFZ-7	110.74	400	0.9	0.13	229	29	349	33	194	14		
		800	2.1	0.21	28.9	2.0	130.5	3.4	54.6	3.8		
		1200	0.0	0.10	-	-	-	-	0.1	0.2	249	15
GFZ-8	502.7	20	10.2	0.53	3.96	0.07	102.9	0.9	10.16	0.89	10.16	0.89
GFZ-9	201.19	400	1.1	0.11	97.7	5.9	207.3	7.2	99.1	7.5		
		600	3.7	0.28	32.69	0.61	133.7	2.7	111.2	8.1		
		800	12.7	0.92	10.00	0.16	110.3	0.7	89.2	6.7		
		1200	10.1	1.1	6.21	0.16	105.7	1.6	32.8	3.8	332	13
GFZ-10	201.1	400	2.4	0.19	57.3	3.1	162.8	3.4	129.2	7.3		
		600	5.5	0.32	24.60	0.69	126.5	1.4	118.2	6.7		
		800	10.3	0.61	7.79	0.15	106.6	0.6	50.0	3.2		
		1200	6.6	0.41	6.61	0.20	108.5	0.9	24.0	1.7	321	11
CRPG-1	149.1	820	14.15	0.54	21.7	1.2	122.4	6.5	267	19		

Continued on next page

Table 1 – concluded from previous page

	mass	T	^{20}Ne	2σ	21/20	2σ	22/20	2σ	^{21}Ne*	2σ	sum	2σ
		1260	16.95	0.64	6.22	0.45	104.5	5.4	55.4	7.9	322	21
CRPG-2	83.3	1180	28.0	1.1	14.46	0.79	114.3	6.0	323	25		
		1260	0.03	0.16	12	79	-	-	0.3	2.6	323	26

Table 2: Same as Table 1, but for the fine fraction of CREU-1.

	mass [mg]	T [°C]	^{20}Ne [$\times 10^9$at/g]	2σ	21/20 [$\times 10^{-3}$]	2σ	22/20 [$\times 10^{-3}$]	2σ	^{21}Ne* [$\times 10^6$at/g]	2σ	sum [$\times 10^6$at/g]	2σ
ETH-8	73.38	600	8.59	0.20	40.61	0.34	147.1	1.5	323.4	7.9		
		800	6.78	0.21	6.21	0.18	107.6	1.3	22.1	0.9		
		1750	8.39	0.22	5.20	0.11	108.3	1.2	18.8	0.6	364	12
ETH-9	70.42	600	9.91	0.21	35.20	0.31	142.6	1.1	319.3	7.4		
		800	6.24	0.14	6.00	0.08	106.8	1.2	19.0	0.5		
		1750	8.11	0.16	5.13	0.15	105.7	1.5	17.7	0.6	356	11
SUERC-15	378.6	450	3.17	0.19	58.9	1.5	164.5	5.3	174.6	11.4		
		550	3.84	0.23	28.39	0.75	130.9	4.2	96.4	6.4		
		650	3.88	0.23	10.03	0.32	107.4	3.8	27.0	1.9		
		800	10.41	0.62	6.05	0.17	107.2	3.4	31.8	2.2		
		1350	9.36	0.56	4.62	0.16	104.2	3.3	15.3	1.1	345	13
SUERC-16	237.1	550	0.86	0.05	52.0	1.9	158.5	8.8	41.8	3.2		
		650	2.34	0.14	54.8	1.6	161.7	7.1	119.9	8.3		
		800	2.11	0.13	26.90	0.62	121.5	4.5	49.9	3.2		
		1350	24.5	1.5	8.85	0.20	108.0	4.0	142.2	9.1		
		480	0.73	0.04	10.14	0.81	106.4	5.6	5.2	0.6	359	13
SUERC-17	33	1350	31.6	1.9	15.04	0.29	115.9	1.3	374.9	24.5	375	25
SUERC-18	156.2	1350	26.7	1.6	16.56	0.27	116.2	1.2	357.7	22.5	358	22
SUERC-19	166	1350	25.6	1.5	16.99	0.17	116.8	0.9	352.7	21.6	353	22

Continued on next page

Table 2 – concluded from previous page

	mass	T	^{20}Ne	2σ	21/20	2σ	22/20	2σ	^{21}Ne*	2σ	sum	2σ
GFZ-11	100.24	400	0.96	0.13	152.0	16.0	263.0	18.0	142.9	13.7		
		600	3.30	0.27	38.3	1.2	139.6	3.1	116.6	8.6		
		800	12.57	0.94	7.87	0.16	108.2	1.0	61.8	4.8		
		1200	3.33	0.30	5.66	0.34	104.3	4.1	9.0	1.2	330	17

Table 3: Same as Tables 1 and 2, but for CRONUS-A.

	mass	T	^{20}Ne	2σ	21/20	2σ	22/20	2σ	^{21}Ne*	2σ	sum	2σ
	[mg]	[°C]	[$\times 10^9$at/g]		[$\times 10^{-3}$]		[$\times 10^{-3}$]		[$\times 10^6$at/g]		[$\times 10^6$at/g]	
BGC-10	137.7	390	2.21	0.72	69.28	22.43	172	59	144.4	8.2		
		780	11.48	1.10	19.13	1.63	119	11	183.0	11.3		
		1140	1.65	0.35	9.53	2.16	110	36	10.6	1.8	338	14
BGC-11	105.9	390	2.19	0.52	72.48	16.99	179	49	150.2	8.1		
		780	9.72	0.77	21.06	1.67	126	12	173.2	8.4		
		1140	1.33	0.65	11.39	5.70	101	69	11.1	2.6	334	12
BGC-12	122.5	370	2.68	1.24	50.59	23.39	140	72	124.7	6.5		
		740	9.86	0.33	22.09	0.76	124	8	192.0	4.5		
		1140	2.11	0.63	12.35	3.72	122	43	20.0	2.5	337	8
BGC-13	107.5	370	4.26	1.59	33.44	12.55	124	50	126.3	6.9		
		740	11.27	1.11	20.37	2.07	118	15	195.1	7.7		
		1140	3.70	1.79	6.44	3.13	97	54	12.8	5.6	334	12
BGC-14	66.7	370	4.18	0.89	32.74	7.03	138	46	123.7	5.5		
		740	10.43	0.46	21.66	1.10	123	16	195.2	8.5		
		1140	2.13	0.89	11.16	4.81	128	77	17.2	3.6	336	11
BGC-15	138.3	370	3.20	0.73	42.97	9.58	139	41	127.1	10.0		
		740	10.24	0.42	22.06	0.68	123	8	193.1	8.7		
		1140	2.33	0.57	9.84	2.47	126	39	15.7	2.3	336	13
BGC-16	167.8	390	4.53	0.63	33.39	4.36	135	21	138.3	8.1		
		780	12.32	0.68	19.17	0.79	118	7	199.3	10.2		

Continued on next page

Table 3 – concluded from previous page

	mass	T	^{20}Ne	2σ	21/20	2σ	22/20	2σ	^{21}Ne*	2σ	sum	2σ
		1140	1.93	0.52	10.52	2.91	122	46	14.0	2.1	352	13
BGC-17	138.1	370	2.57	0.61	42.68	10.09	155	50	102.0	5.4		
		740	11.97	0.64	21.61	0.99	123	9	226.3	12.9		
		1140	2.96	0.56	10.70	2.10	110	32	22.3	2.8	351	14
BGC-18	144.8	370	2.47	0.39	42.38	6.57	153	56	97.0	8.0		
		740	11.29	0.45	22.40	0.93	126	11	219.1	7.2		
		1140	3.93	0.50	9.24	1.26	114	26	24.8	2.7	341	11
CRPG-3	37.2	1200	13.21	0.64	26.43	1.75	138	9	311.2	27.6		
		1280	0.32	0.35	2.33	7.29	< DL	0	< DL	2.3	311	28

References

Amidon, W. H., Farley, K. A., 2012. Cosmogenic ^{3}He and ^{21}Ne dating of biotite and hornblende. Earth and Planetary Science Letters 313-314 (0), 86 – 94.

Balco, G., Shuster, D. L., 2009a. ^{26}Al-^{10}Be-^{21}Ne burial dating. Earth and Planetary Science Letters 286, 570–575.

Balco, G., Shuster, D. L., 2009b. Production rate of cosmogenic ^{21}Ne in quartz estimated from ^{10}Be, ^{26}Al, and ^{21}Ne concentrations in slowly eroding Antarctic bedrock surfaces. Earth and Planetary Science Letters 281, 48–58.

Baur, H., 1980. Numerische Simulation und praktische Erprobung einer rotationssymmetrischen Ionenquelle für Gasmassenspektrometer. Ph.D. Thesis, ETH-Zürich No. 6596.

Baur, H., 1999. A noble-gas mass spectrometer compressor source with two orders of magnitude improvement in sensitivity. Eos, Transactions of the American Geophysical Union 80, F1118.

Codilean, A. T., Bishop, P., Stuart, F. M., Hoey, T. B., Fabel, D., Freeman, S. P. H. T., 2008. Single-grain cosmogenic ^{21}Ne concentrations in fluvial sediments reveal spatially variable erosion rates. Geology 36, 159–162.

Dunai, T. J., González López, G. A., Juez-Larré, J., apr 2005. Oligocene Miocene age of aridity in the Atacama Desert revealed by exposure dating of erosion-sensitive landforms. Geology 33, 321–324.

Dunai, T. J., Stuart, F. M., 2009. Reporting of cosmogenic nuclide data for exposure age and erosion rate determinations. Quaternary Geochronology 4 (6), 437–440.

Fujioka, T., Chappell, J., Honda, M., Yatsevich, I., Fifield, K., Fabel, D., 2005. Global cooling initiated stony deserts in central Australia 2-4 Ma, dated by cosmogenic ^{21}Ne-^{10}Be. Geology 33, 993.

Goethals, M. M., Niedermann, S., Hetzel, R., Fenton, C. R., 2009. Determining the impact of faulting on the rate of erosion in a low-relief landscape: A case study using in situ produced ^{21}Ne on active normal faults in the Bishop Tuff, California. Geomorphology 103, 401–413.

Heber, V. S., Wieler, R., Baur, H., Olinger, C., Friedmann, T. A., Burnett, D. S., 2009. Noble gas composition of the solar wind as collected by the Genesis mission. Geochimica et Cosmochimica Acta 73, 7414–7432.

Kober, F., Alfimov, V., Ivy-Ochs, S., Kubik, P. W., Wieler, R., 2011. The cosmogenic ^{21}Ne production rate in quartz evaluated on a large set of existing ^{21}Ne-^{10}Be data. Earth and Planetary Science Letters 302, 163–171.

Kober, F., Ivy-Ochs, S., Leya, I., Baur, H., Magna, T., Wieler, R., Kubik, P. W., 2005. In situ cosmogenic ^{10}Be and ^{21}Ne in sanidine and in situ cosmogenic ^{3}He in Fe Ti-oxide minerals. Earth and Planetary Science Letters 236, 404–418.

Kober, F., Ivy-Ochs, S., Zeilinger, G., Schlunegger, F., Kubik, P. W., Baur, H., Wieler, R., 2009. Complex multiple cosmogenic nuclide concentration and histories in the arid Rio Lluta catchment, northern Chile. Earth Surface Processes and Landforms 34 (3), 398–412.

Lal, D., 1991. Cosmic ray labeling of erosion surfaces: *in situ* nuclide production rates and erosion models. Earth and Planetary Science Letters 104, 424–439.

McIntyre, G. A., Brooks, C., Compston, W., Turek, A., 1966. The Statistical Assessment of Rb-Sr Isochrons. Journal of Geophysical Research 71, 5459–5468.

Middleton, J., Ackert Jr., R., Mukhopadhyay, S., 2012. Pothole and channel system formation in the mcmurdo dry valleys of antarctica: New insights from cosmogenic nuclides. Earth and Planetary Science Letters 355-356, 341 – 350.

Niedermann, S., 2002. Cosmic-Ray-Produced Noble Gases in Terrestrial Rocks: Dating Tools for Surface Processes. In: Porcelli, D., Ballentine, C. J., Wieler, R. (Eds.), Noble Gases in Geochemistry and Cosmochemistry. Vol. 47 of Reviews in Mineralogy and Geochemistry. Mineralogical Society of America, pp. 731–784.

Niedermann, S., Bach, W., Erzinger, J., 1997. Noble gas evidence for a lower mantle component in MORBs from the southern East Pacific Rise: Decoupling of helium and neon isotope systematics. Geochimica et Cosmochimica Acta 61, 2697–2715.

Niedermann, S., Graf, T., Kim, J., Kohl, C., Marti, K., Nishiizumi, K., 1994. Cosmic-ray-produced ^{21}Ne in terrestrial quartz: the neon inventory of Sierra Nevada quartz separates. Earth and Planetary Science Letters 125 (1-4), 341–355.

Niedermann, S., Graf, T., Marti, K., 1993. Mass spectrometric identification of cosmic-ray-produced neon in terrestrial rocks with multiple neon components. Earth and Planetary Science Letters 118, 65–73.

Poreda, R. J., Cerling, T. E., 1992. Cosmogenic neon in recent lavas from the western United States. Geophysical Research Letters 19, 1863–1866.

Schäfer, J. M., Ivy-Ochs, S., Wieler, R., Leya, I., Baur, H., Denton, G. H., Schlüchter, C., 1999. Cosmogenic noble gas studies in the oldest landscape on earth: surface exposure ages of the Dry Valleys, Antarctica. Earth and Planetary Science Letters 167, 215–226.

427 Shuster, D., Farley, K., 2005. Diffusion kinetics of proton-induced ^{21}Ne, ^{3}He, and ^{4}He in
428 quartz. Geochimica et Cosmochimica Acta 69, 2349–2359.

429 Stuart, F. M., Dunai, T. J., 2009. Editorial. Quaternary Geochronology 4 (6), 435 – 436,
430 advances in Cosmogenic Isotope Research from CRONUS-EU.

431 Vermeesch, P., Fenton, C. R., Kober, F., Wiggs, G. F. S., Bristow, C. S., Xu, S., 2010. Sand
432 residence times of one million years in the Namib Sand Sea from cosmogenic nuclides.
433 Nature Geoscience 3, 862–865.

434 Zimmermann, L., Blard, P.-H., Burnard, P., Medynski, S., Pik, R., Puchol., N., in press. A
435 new single vacuum furnace design for cosmogenic ^{3}He dating. Geostandards and Geoana-
436 lytical Research.